Structural, Morphological and Thermal Decomposition Studies of Calcium and Hafnium Modified $BaTiO_3$ Electro Ceramics

Jude Fernandez
Noorul Islam College of Engineering: Noorul Islam Centre For Higher Education
B Bindhu (bindhu.krishna80@gmail.com)
Noorul Islam College of Engineering: Noorul Islam Centre For Higher Education https://orcid.org/0000-0002-0577-0923
M. Prabu
Noorul Islam College of Engineering: Noorul Islam Centre For Higher Education
KY Sandhya
Indian Institute of Space Science and Technology

Research Article

Keywords: Sol-gel, ferroelectric, crystallize, tetragonal, phase boundary

Posted Date: February 26th, 2021

DOI: https://doi.org/10.21203/rs.3.rs-243264/v1

Abstract

Calcium and hafnium co-doped barium titanate could be used as a replacement for lead zirconate titanate, which is a lead-based ferroelectric material. Solid state reaction accompanied by the usual sintering technique is the classical ceramic-processing method, which demands a lot of time and effort. The present work aims to make the process a lot easier and quicker by employing a modified sol-gel combustion technique to synthesize polycrystalline $Ba_{0.85}Ca_{0.15}Ti_{(1-x)}Hf_xO_3$ (x=0.00, 0.05, 0.10, 0.15) electro ceramics . The molar ration is fixed at 1:1 for metal and citric acid at pH ~ 1. It was found that $Ba_{0.85}Ca_{0.15}Ti_{(1-x)}Hf_xO_3$ (where x=0.00, 0.05, 0.10, 0.15) crystallizes completely at around 1000 °C which is much lower than traditional methods. The structure supposedly displays a tetragonal symmetry with the P4mm space group as confirmed through x-ray diffraction (XRD) and Raman spectroscopy.

1. Introduction

Life in the 21st century is largely influenced by Artificial Intelligence (AI), which means we live in a data-driven world. Active Internet users worldwide is roughly 4.57 billion as of 2020, and each of them creates ~1.7 MB of data, on average, every second [1–5]. With the growing number of Internet-of-Things (IoT) devices and rise of smart cities, complemented by 5G networks, data generation per day is projected to increase to 463 exabytes by 2025 [6–12]. Furthermore, the increasing number of remote jobs in the ongoing pandemic allows people to limit physical contact with co-workers and things (especially touch screen gadgets) [10]. As tasks are becoming largely data intensive, the necessity of increased computational cost to run capable hardware becomes a hurdle. In this scenario, the emergence of new ferroelectric materials appears as a light in the darkness [11–15].

Although ferroelectric materials have been around for a century, they have recently attracted more attention with the growing popularity of multifunctional materials. They are excellent options for low-power sensors and non-volatile memories [9]. The ferroelectric materials market was largely dominated by lead zirconate titanate (PZT) ceramics for decades. Due to the hazards associated with lead for both humans and the environment, many nations have banned its usage across various industries [16–20]. Manufacturers of smart devices using the ferroelectric property of PZT, which was described as a possible carcinogen, were therefore forced to look for alternatives. Barium titanate is one of the few ceramics known to exhibit excellent ferroelectric properties. It was one of the most important ferroelectric oxides used in the electronic industry before the invention of PZT [21–24]. The d33 coefficients and ferroelectric properties of doped barium titanate are comparable to those of PZT. In 2008, with the discovery of high d33 coefficients in calcium and zirconium (Zr) co-doped barium titanate, scientists again started investigating the material [25–30]. This work is an attempt to obtain improved properties in doped barium titanate by replacing Zr with hafnium (Hf) using a novel sol-gel synthesis technique. Solid state methods used traditionally requires very high calcination temperatures of up to 1300 °C and extremely high sintering temperatures around 1600 °C. Both the metals possess similar atomic radii due to lanthanide contraction, and hence similar properties are expected.

In this work, a comparatively easy synthesis technique for the production of $Ba_{0.85}Ca_{0.15}Ti_{(1-x)}Hf_xO_3$ (x=0.00, 0.10, 0.15) ceramics is proposed. The structural characteristics were analysed using x-ray diffraction (XRD). Thermal decomposition studies of the as-prepared gel were carried out using thermogravimetric/differential thermal analysis (TG/DTA). Scanning electron microscopy (SEM) was used to study the morphology of the ceramic samples, and any unwanted functional groups were confirmed using Fourier transform infrared spectroscopy (FTIR). Raman spectroscopy was used to confirm structural symmetry as well as the presence of any multiple phases in the structure.

2. Materials And Methods

With a magnetic stirrer, citric acid anhydrous (99.5% AR-Sisco Research Laboratories Pvt. Ltd.) was stirred in de-ionized water until it was completely dissolved. Barium nitrate (99.0% AR-Sisco Research Laboratories Pvt. Ltd.) and titanium isopropoxide (98.0%-Sisco Research Laboratories Pvt. Ltd.) were then added to the solution, followed by calcium nitrate tetrahydrate (99.0% AR-Sisco Research Laboratories Pvt. Ltd.) and hafnium dichloride oxide octahydrate (99.9%-Alfa Aesar). Nitric acid (69.0%-Merck) was added dropwise to adjust the pH at around 1, and the solution was stirred continuously at 100 °C. After 4 hours, the solution would boil and froth before turning into a dark brown powder as a result of ignition. The powder was calcined in air at 1000 °C in a high-temperature muffle furnace to remove organic compounds and vaporous impurities. X-ray diffraction (Bruker D2 Phaser 2^{nd} generation diffractometer) was used to analyse the crystal phase of the material with Cu K_α radiation of 1.54 Å. TGA/DTA analysis was conducted between 0 °C and 100 °C. Fourier transform infrared spectroscopy (Bruker Alpha II) was done between 500 cm^{-1} and 4000cm^{-1}. Raman spectroscopy (EZ Raman high-performance series II) was used to analyse the structural phases in the material. Carl Zeiss EVO 18 scanning electron microscope (SEM) was used to obtain the microscopic images of all samples.

3. Results And Discussion

3.1 XRD analysis

X-ray diffraction patterns of $Ba_{0.85}Ca_{0.15}Ti_{(1-x)}Hf_x$ (where x=0.00, 0.05, 0.10, 0.15) are shown in Figure 1. For all the compositions, the structure crystallizes with the tetragonal symmetry having the P4mm space group. All the obtained peaks were compared with the reference file available in the Joint Committee on Powder Diffraction Standards (JCPDS) database with COD ID: 04-019-9410. It was observed that a pure perovskite structure without any secondary phase was obtained. A well-defined peak was obtained at 30° which confirms the formation of the perovskite phase. It is very clear from the patterns that both Hf and Ca have completely diffused into the corresponding lattice sites of barium titanate. The additional peaks obtained for BCTH5 and BCTH15 may be due to trace amounts of BaO phase formed during calcination.

3.2 TG/DTA analysis

Figure 2 shows the thermal decomposition behaviour of BCTH10. It portrays the differential thermal and thermogravimetric analyses of the BCTH10 sample at a heating rate of 20 °C/min. As seen in the figure, the curve presents more than one peak for both endothermic and exothermic effects. This is due to the dehydration of absorbed water present in the ceramic combined with the removal of other organic compounds. The DTA curve presents an exothermic peak at 375 °C, probably due to the removal of water and the resultant weight loss of around 13%. The peaks at 500 °C, 570 °C, 603 °C, and 630 °C, due to the decomposition of metal complex, removal of organic compounds, and phase formation, contributed to a further weight loss of 37%. The weight loss after 630 °C is negligible, as confirmed by the straight line in the TG curve after this point.

3.3 FTIR analysis

Figure 3 shows the Fourier transform infrared spectra of the BCTH samples. A broad band at 570 cm^{-1} confirms the formation of metal oxide. The stretching vibration of Ti-O and Hf-O is confirmed by the peak at 565 cm^{-1}. The peaks at 2364 cm^{-1} for the BCTH10 and BCTH15 samples are due to carbon dioxide, which may have formed as a direct result of the measuring conditions. The BCTH0 curve has no peak at 1684 cm^{-1} whereas the Hf doped BCTH shows a new peak at the value mentioned and may probably be due to the presence of hafnium. The peak may have occurred for all other samples due to the presence of a C=O carbonyl group which formed during the synthesis as a result of decomposition of hafnium dichloride oxide octahydrate which is an alkoxide. The hygroscopic nature of the material increases with increase in hafnium concentration. The peaks at 3750 cm^{-1} and 3884 cm^{-1} further supports the argument which occurred due to O-H stretching mode of water molecule.

3.4 Morphological studies

The scanning electron microscopy (SEM) images obtained for all the samples are shown in Figure 4. The SEM images clearly show that the particles undergo agglomeration. All the grains in the sample possess polyhedral geometry. The BCTH10 sample has the largest grain size. Larger grain sizes potentially yield better ferroelectric and piezoelectric properties.

3.5 Raman spectroscopic analysis

The materials in the region of 150–1000 cm^{-1} were analysed using Raman spectroscopy, a well-known tool to understand the physics of ferroelectric materials from their lattice-dynamics coupling. Moreover, Raman spectroscopy has a lower time scale as opposed to x-ray diffraction and presents a good structural fingerprint of the material under consideration. All the studied samples exhibit a tetragonal structure. This is confirmed by the peaks at 170 cm^{-1} and 247cm^{-1}, as well as the prominent peak at 514 cm^{-1}. The broad peak around 836 cm^{-1} is due to the presence of several dissimilar atoms at the A and B sites.

4. Conclusions

BCTH ceramics were successfully synthesized using the sol-gel technique. The structural parameters, which were studied using x-ray diffraction (XRD), confirmed the presence of tetragonal symmetry in all the compositions with the P4mm space group. Thermogavimetric and differential thermal analysis (TG/DTA) identified the material phase formation temperature at 1000 °C. Fourier transform infrared spectroscopy (FTIR) analysis showed that the material is free of unwanted functional groups. The morphology and shape of all the grains in the samples appeared to be polyhedral. The BCTH10 sample has the greatest grain size among all samples. In addition to XRD analysis, Raman spectroscopy showed that all the samples possess tetragonal phase with the P4mm space group.

Declarations

Funding: This research did not receive any specific grant from funding agencies in the public, commercial, or not-for-profit sectors.

Acknowledgements

The authors are grateful to the Central Laboratory for Instrumentation and Facilitation (CLIF), University of Kerala, Thiruvananthapuram for providing characterization facilities.

Declaration of Interest

The authors declare that they have no known competing financial interests or personal relationships that could have appeared to influence the work reported in this paper

References

1. Suryasa, I.G.P.A. Prayoga, I.W.A. Werdistira, Attitudes toward the use of Internet for students. Int. J. Phys. Sci. Eng. 2 (2018) 32–38.
2. J.D. Schnebly, Distilling Public Data from Multiple Sources for Cybersecur. Appl. Diss. 2020.
3. S.S. Martins, C. Wernick, Regional differences in residential demand for very high bandwidth broadband Internet in 2025. Telecommun. Policy 45 (2021) 102043.
4. A. Clemm, M.F. Zhani, R. Boutaba, Network management 2030: Operations and control of network 2030 services. J. Netw. Syst. Manag. (2020) 1–30.
5. Z. Allam, Z.A. Dhunny, "On big data, artificial intelligence and smart cities". Cities 89 (2019): 80–91.
6. I. A. T. Hashem, V. Chang, N. B. Anuar, K. Adewole, I. Yaqoob, A. Gani, E. Ahmed, H. Chiroma, "The role of big data in smart city". Int. J. of Inf. Manage. 36.5 (2016): 748–758.
7. D.G. Broo, U. Boman, M. Törngren, "Cyber-physical Systems Research and Education in 2030: Scenarios and Strategies". J. of Ind. Inf. Integr. (2020): 100192.
8. S. Bhattacharya, S.R.K. Somayaji, T.R. Gadekallu, M. Alazab, P.K.R. Maddikunta, "A review on deep learning for future smart cities". Internet Technol. Lett. (2020): e187.

9. D. Soeiro, “Smart Cities, Well-Being and Good Business: The 2030 Agenda and the Role of Knowledge in the Era of Industry 4.0”. Knowl. People and Digital Transform. Springer, Cham, 2020. 55–67.
10. A century of ferroelectricity. Nat. Mater. 19, 129 (2020).
11. Y. Pan, "Heading toward artificial intelligence 2.0". Eng. 2.4 (2016): 409–413.
12. Z. Allam, Z.A. Dhunny, "On big data, artificial intelligence and smart cities". Cities 89 (2019): 80–91.
13. D.W. Denno, R. Surujnath, "Rise of the Machines: Artificial Intelligence, Robotics, and the Reprogramming of Law (Symp. Foreword)". (October 31, 2019). Vol. 88. 2019.
14. R. Ali, G.J. Hou, Z.G. Zhu, Q.B. Yan, Q.R. Zheng, G. Su, "Predicted lead-free perovskites for solar cells". Chem. of Mater. 30.3 (2018): 718–728.
15. M.D. Maeder, D. Damjanovic, N. Setter, "Lead free piezoelectric materials". J. of Electroceram. 13.1-3 (2004): 385–392.
16. Damjanovic, N. Klein, J. Li, V. Porokhonskyy, "What can be expected from lead-free piezoelectric materials?". Funct. Mater. Lett. 3.01 (2010): 5–13.
17. P.K. Panda, B. Sahoo, "PZT to lead free piezo ceramics: a review". Ferroelectr. 474.1 (2015): 128–143.
18. M. Acosta, N. Novac, V. Rojas, S. Patel, R. Vaish, J. Koruza, G.A. Rossetti Jr. J.Rödel, "BaTiO3-based piezoelectrics: Fundamentals, current status, and perspectives". Appl. Phys. Rev. 4.4 (2017): 041305.
19. K. Uchino, E. Sadanaga, T. Hirose. "Dependence of the crystal structure on particle size in barium titanate". J. of the Am. Ceram. Soc. 72.8 (1989): 1555–1558.
20. M.H. Lee, D.J. Kim, J.S. Park, S.W. Kim, T.K. Song, M.H. Kim, W.J. Kim, D. Do, I.K. Jeong, "High-performance lead-free piezoceramics with high curie temperatures". Adv. Mater. 27.43 (2015): 6976–6982.
21. S. Sharma, K. Shamim, A. Ranjan, R. Rai, P. Kumari, S. Sinha, "Impedance and modulus spectroscopy characterization of lead free barium titanate ferroelectric ceramics". Ceram. Int. 41.6 (2015): 7713–7722.
22. M.M Vijatović, J. D. Bobić, B. D. Stojanović, "History and challenges of barium titanate: Part II". Sci. of Sinter. 40.3 (2008): 235–244.
23. Q. Lou, X. Shi, X. Ruan, J. Zeng, Z. Man, L. Zheng, C.H. Park, G. Li (2018), “Ferroelectric properties of Li-doped BaTiO3 ceramics”. J. of the Am. Ceram. Soc. 101(8), 3597–3604.
24. T. Zaman, M.K. Islam, M.A. Rahman, A. Hussain, M.A. Matin, M.S. Rahman (2019), “Mono and co-substitution of Sr2+ and Ca2+ on the structural, electrical and optical properties of barium titanate ceramics”. Ceram. Int. 45(8), 10154–10162.
25. A.A Kholodkova, M.N. Danchevskaya, Y.D. Ivakin, G.P. Muravieva, A.D. Smirnov, V.P. Tarasovskii, S.G. Ponomarev, A.S. Fionov, V.V. Kolesov (2018), Properties of barium titanate ceramics based on powder synthesized in supercritical water. Ceram. Int. 44(11), 13129–13138.
26. Y. Huang, C. Zhao, J. Yin, X. Lv, J. Ma, J. Wu, "Giant electrostrictive effect in lead-free barium titanate-based ceramics via A-site ion-pairs engineering". J. of Mater. Chem. *A.* 7.29 (2019): 17366–17375.

27. C. Zhao, B. Wu, H.C. Thong, J. Wu, "Improved temperature stability and high piezoelectricity in lead-free barium titanate-based ceramics". J. of the Eur. Ceram. Soc. 38.16 (2018): 5411–5419.
28. S. Sharma, K. Shamim, A. Ranjan, R. Rai, P. Kumari, S. Sinha, "Impedance and modulus spectroscopy characterization of lead free barium titanate ferroelectric ceramics". Ceram. Int. 41.6 (2015): 7713–7722.
29. C. Zhao, H. Wu, F. Li, Y. Cai, Y. Zhang, D. Song, J. Wu, X. Lyu, J. Yin, D. Xiao, J. Zhu, S.J. Pennycook, "Practical high piezoelectricity in barium titanate ceramics utilizing multiphase convergence with broad structural flexibility". J. of the Am. Chem. Soc. 140.45 (2018): 15252–15260.
30. H. Nagata, M. Yoshida, Y. Makiuchi, T. Takenaka, "Large piezoelectric constant and high Curie temperature of lead-free piezoelectric ceramic ternary system based on bismuth sodium titanate-bismuth potassium titanate-barium titanate near the morphotropic phase boundary". Jpn. J. of Appl. Phys. 42.12R (2003): 7401.

Figures

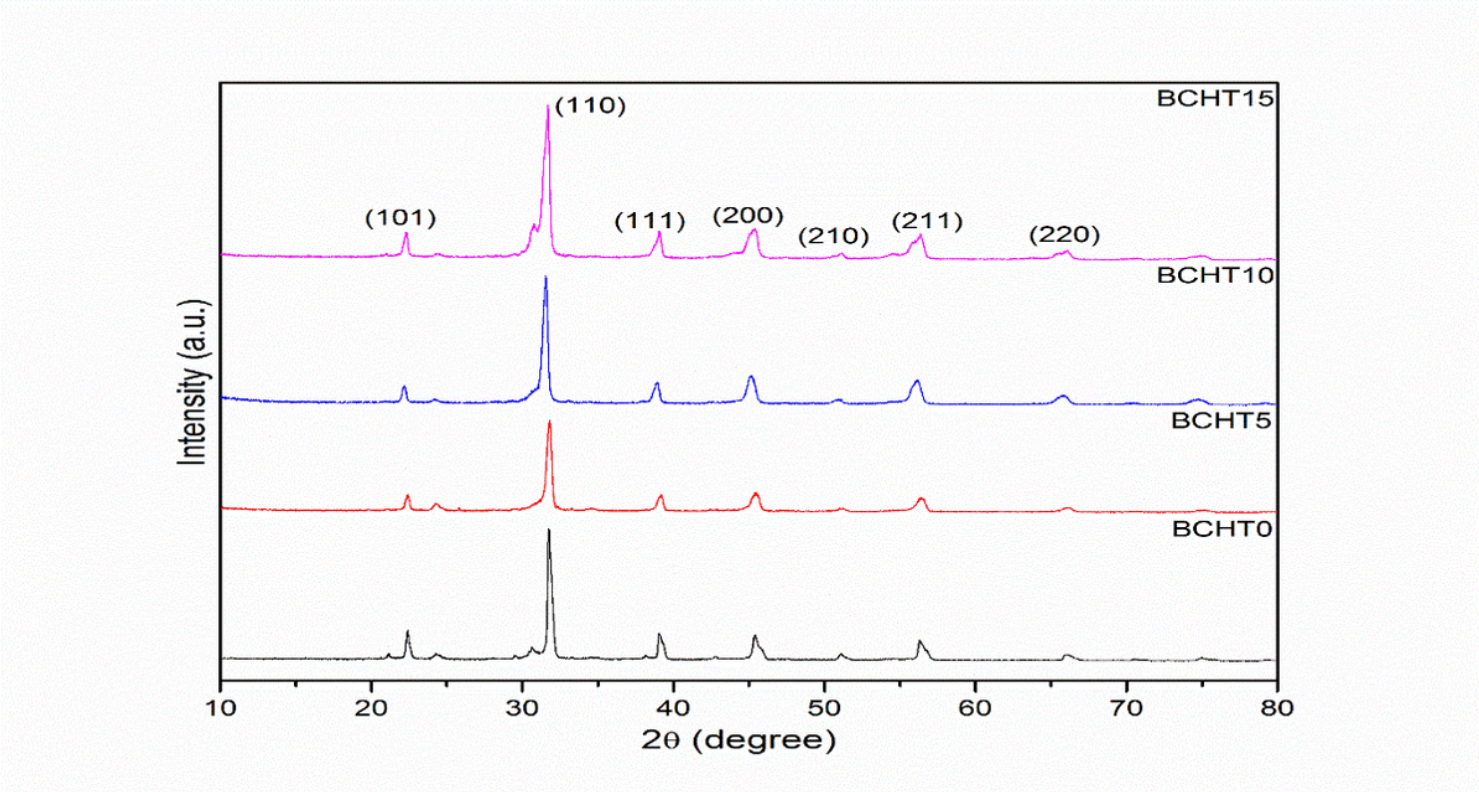

Figure 1

Room temperature XRD pattern of Ba0.85Ca0.15Ti(1-x)Hfx (x=0.00, 0.05, 0.10, 0.15)

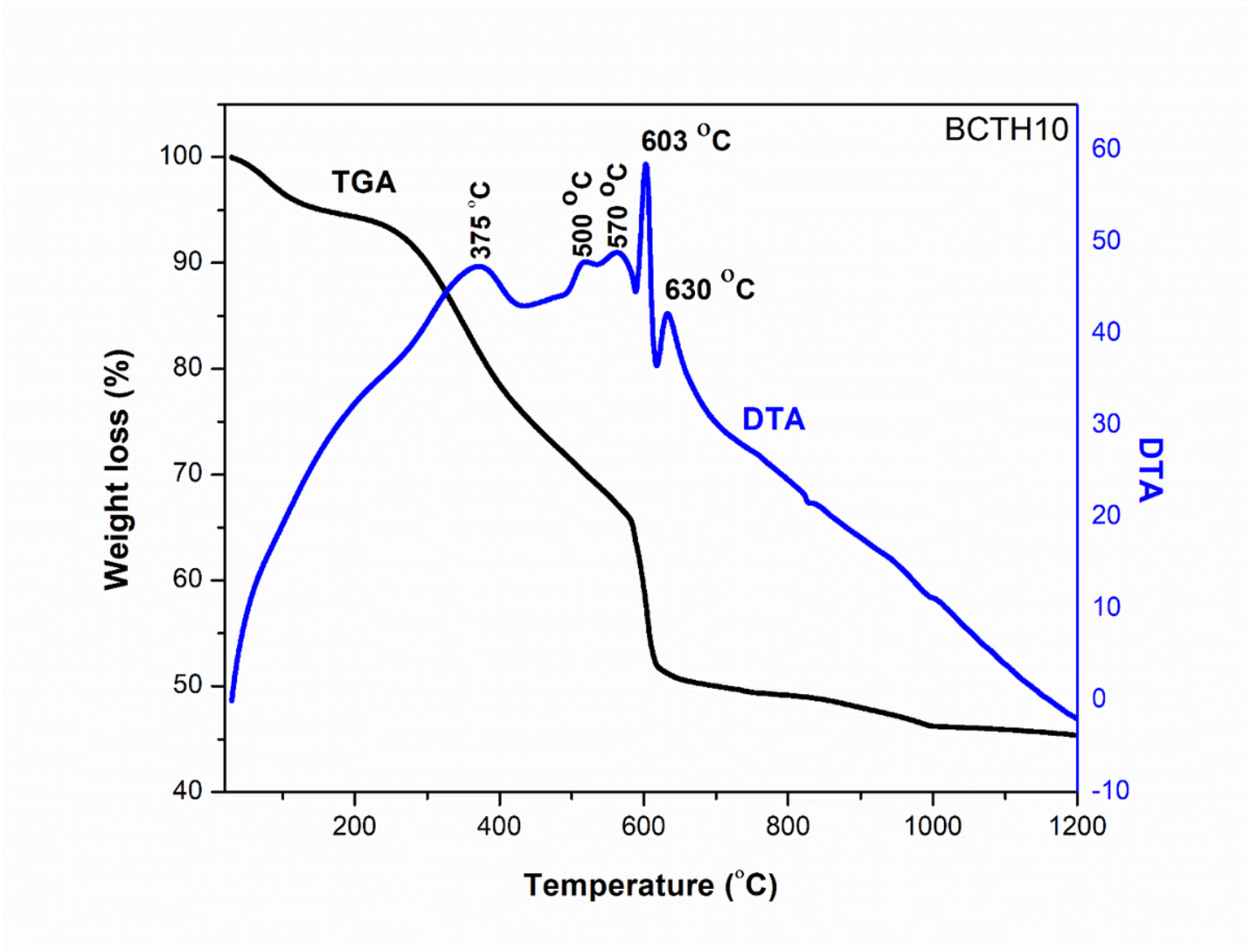

Figure 2

Thermogravimetric analysis/Differential thermal analysis of BCTH10 ceramic sample

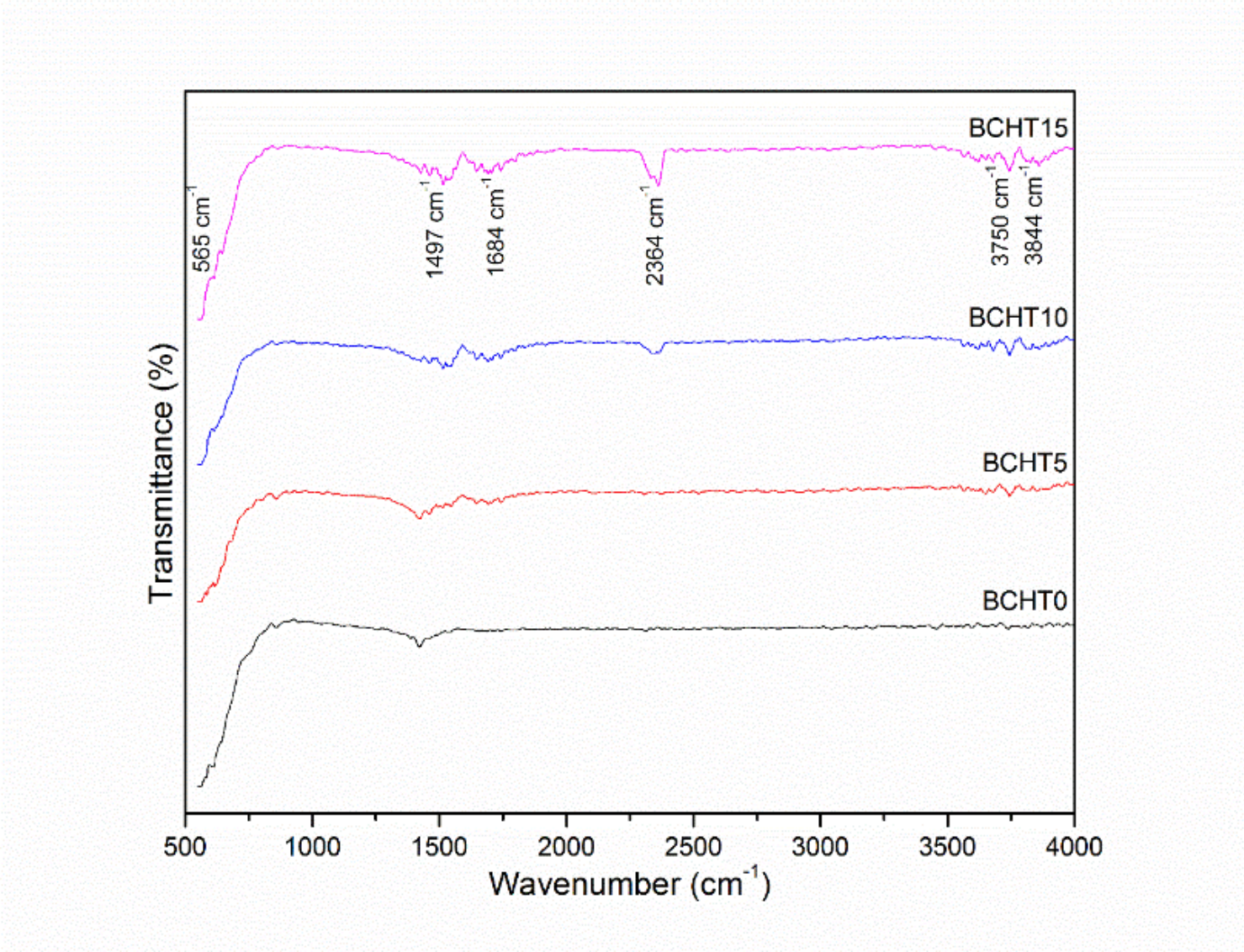

Figure 3

Fourier transform infrared spectra of BaCaTi(1-x)HfxO3 (where x=0.00, 0.05, 0.10, 0.15)

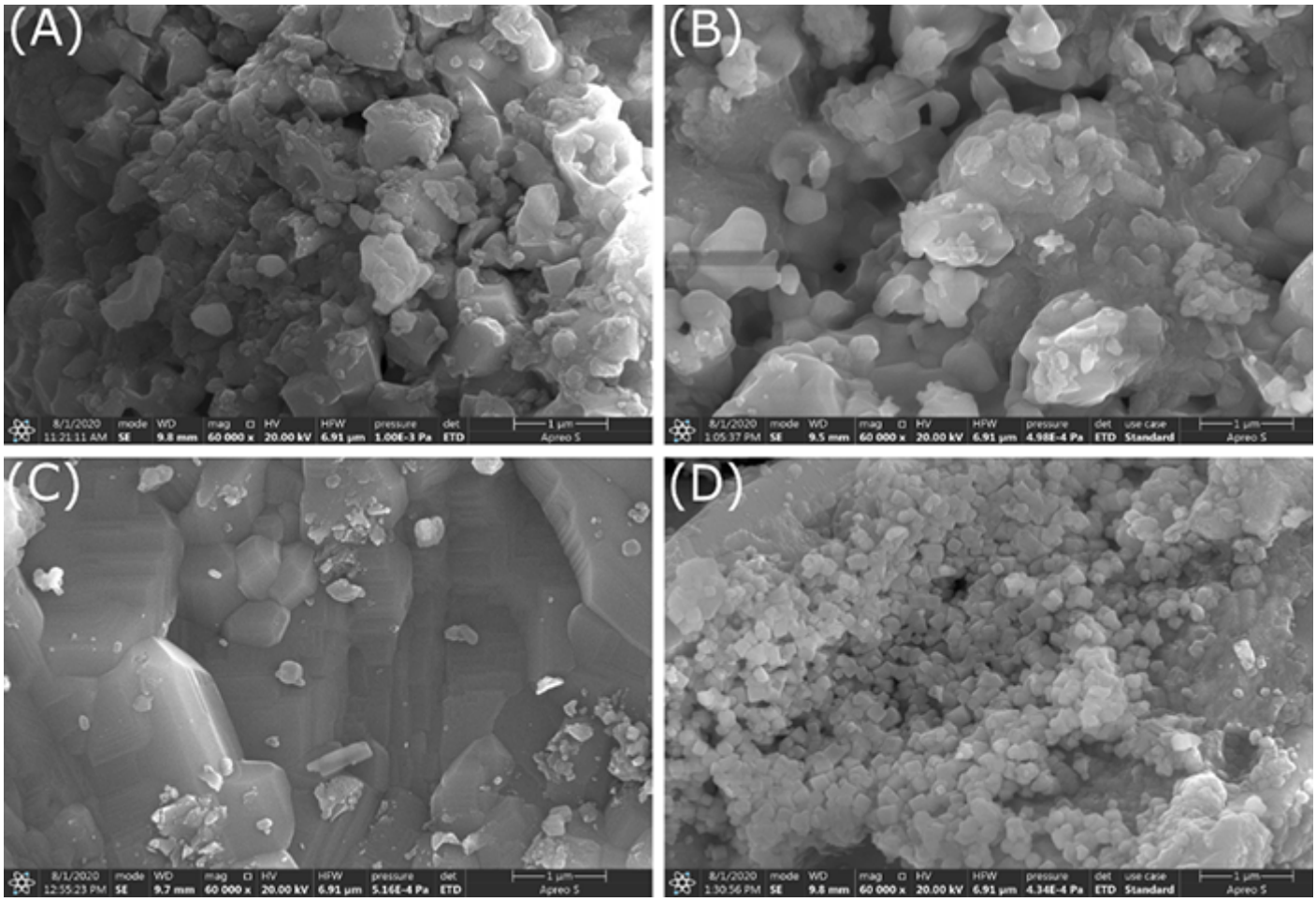

Figure 4

Scanning electron microscopy micrographs of (A) BCTH0, (B) BCTH5, (C) BCTH10, (D) BCTH15

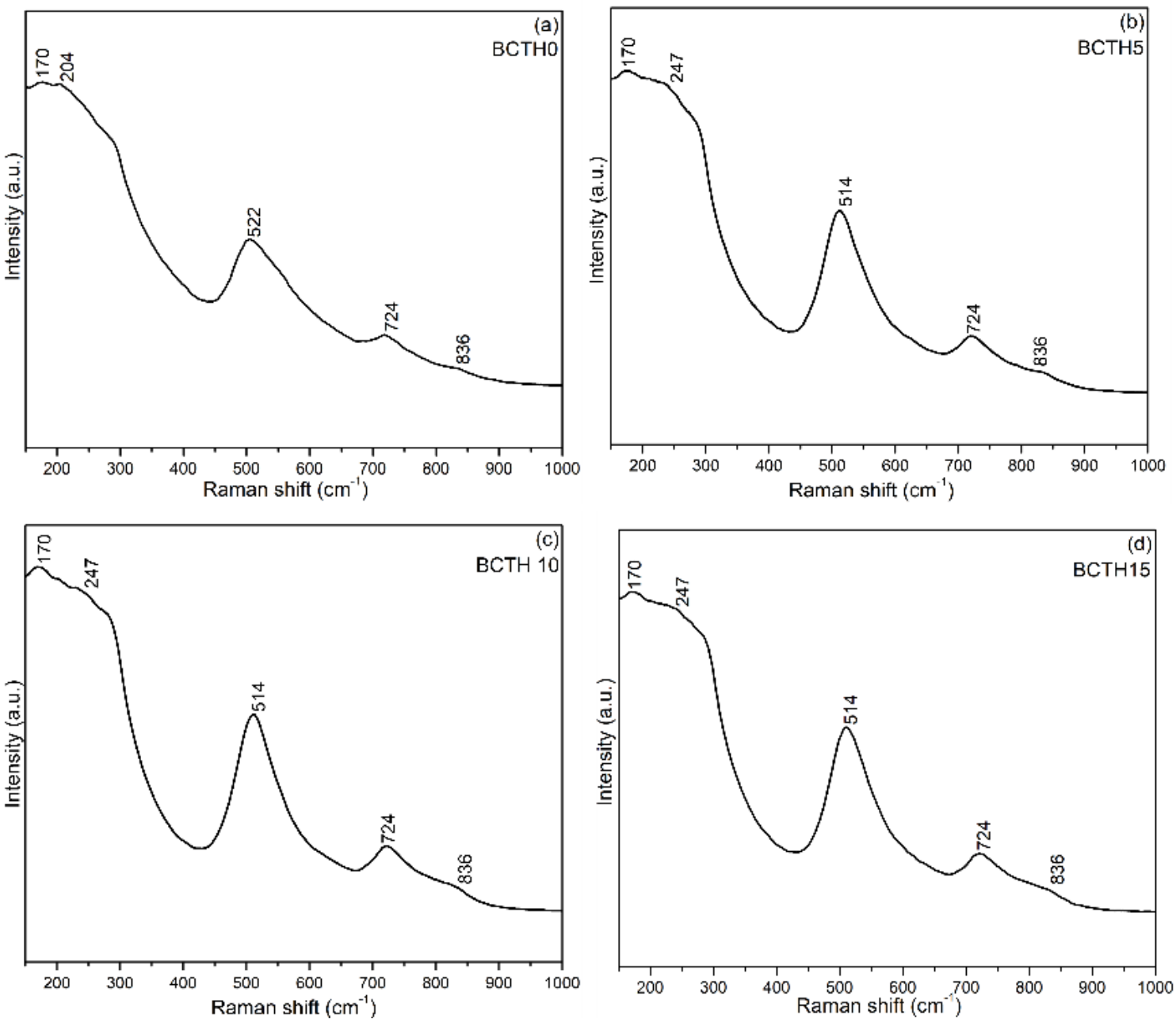

Figure 5

Raman spectra of (a) BCTH0, (b) BCTH5, (c) BCTH 10 and BCTH 15